Wang *et al.*
Biotechnology for Biofuels and Bioproducts (2022) 15:91
https://doi.org/10.1186/s13068-022-02190-2

Biotechnology for Biofuels and Bioproducts

RESEARCH Open Access

In situ carbon dioxide capture to co-produce 1,3-propanediol, biohydrogen and micro-nano calcium carbonate from crude glycerol by *Clostridium butyricum*

Xiao-Li Wang, Jin-Jie Zhou, Sheng Liu, Ya-Qin Sun and Zhi-Long Xiu*

Abstract

Background: Climate change caused by greenhouse gas emission has become a global hot topic. Although biotechnology is considered as an environmentally friendly method to produce chemicals, almost all biochemicals face carbon dioxide emission from inevitable respiration and energy metabolism of most microorganisms. To cater for the broad prospect of biochemicals, bioprocess optimization of diverse valuable products is becoming increasingly important for environmental sustainability and cleaner production. Based on $Ca(OH)_2$ as a CO_2 capture agent and pH regulator, a bioprocess was proposed for co-production of 1,3-propanediol (1,3-PDO), biohydrogen and micro-nano $CaCO_3$ by *Clostridium butyricum* DL07.

Results: In fed-batch fermentation, the maximum concentration of 1,3-PDO reached up to 88.6 g/L with an overall productivity of 5.54 g/L/h. This productivity is 31.9% higher than the highest value previously reports (4.20 g/L/h). In addition, the ratio of H_2 to CO_2 in exhaust gas showed a remarkable 152-fold increase in the 5 M $Ca(OH)_2$ group compared to 5 M NaOH as the CO_2 capture agent. Green hydrogen in exhaust gas ranged between 17.2% and 20.2%, with the remainder being N_2 with negligible CO_2 emissions. During CO_2 capture in situ, micro-nano calcite particles of $CaCO_3$ with sizes in the range of 300 nm to 20 μm were formed simultaneously. Moreover, when compared with 5M NaOH group, the concentrations of soluble salts and proteins in the fermentation broth of 5 M $Ca(OH)_2$ group were notably reduced by 53.6% and 44.1%, respectively. The remarkable reduction of soluble salts and proteins would contribute to the separation of 1,3-PDO.

Conclusions: $Ca(OH)_2$ was used as a CO_2 capture agent and pH regulator in this study to promote the production of 1,3-PDO. Meanwhile, micro-nano $CaCO_3$ and green H_2 were co-produced. In addition, the soluble salts and proteins in the fermentation broth were significantly reduced.

Keywords: 1,3-Propanediol, Micro-nano-$CaCO_3$, Green hydrogen, CO_2 capture, Waste glycerol

*Correspondence: zhlxiu@dlut.edu.cn

School of Bioengineering, Dalian University of Technology, No. 2 Linggong Road, Ganjingzi District, Dalian 116024, Liaoning, People's Republic of China

Graphical Abstract

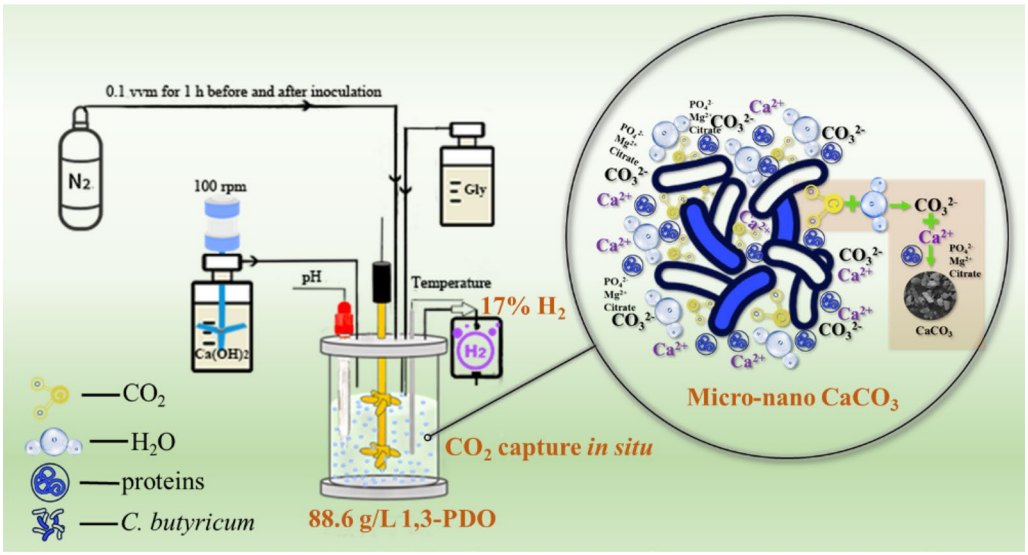

Background

There is a global consensus on the urgent need to reduce carbon footprints to develop a renewable economy and protect our habitable planet. For more than 40,000 years prior to 1912, the atmospheric CO_2 concentration was no higher than 300 ppm, but has risen at an astonishing rate over the last 100 years, reaching 417 ppm by July 2021 [1, 2]. It is estimated that the level of atmospheric CO_2 will up to 500 ppm by 2045, which may pose the most severe threat to the environment and public health [3]. A growing number of countries have declared that they will reduce CO_2 emissions to net-zero within decades, which has greatly encouraged the ambition to tackle climate change [4]. In this case, biotechnology is favored by various countries, which is known as an environmentally friendly method to convert renewable resources to chemicals in a mild reaction. Therefore, biochemicals such as bioethanol, lactic acid, 1,3-PDO, and so on were produced increasingly year by year. However, when considering techno-economic analysis (TEA) of a process, almost all biochemicals production generates greenhouse gas according to their life cycle assessment (LCA)) because of CO_2 from inevitable respiration and energy metabolism of most microorganisms [5]. In detail, the commercial-scale annual production of some biochemicals and the corresponding CO_2 production are presented in Table 1, which are calculated according to the reported microbial metabolic network and the stoichiometry of the reactions. As a result, the annual emission of CO_2 from biochemicals is at least 84.4 million tons, which should be avoided in the future to achieve carbon neutrality. More recently, some proposals for biochemicals production by researchers have focused on optimizing processes for environmental sustainability, identifying cost-effective [12], and new methods (e.g., 3G biorefineries) to capture and convert CO_2 into valuable products [3]. To cater for the broad prospect of biochemicals, the industrially implementable process of

Table 1 Production of some industrial biochemicals by microbial fermentation in major relevant countries and induced CO_2 production in the fermentation

Biochemicals	Production capacity (tons/a year)	Major production Country	induced CO_2 production (tons/a year)	References
Bioethanol	88 million	USA, Brazil &China	84.2 million	[6, 7]
1,3-Propanediol	63,000	USA	118,030	[7, 8]
1,4-Butanediol	105,000	USA, Germany & Italy	13,310	[7, 9]
Butanol	21,460	China	25,480	[10, 11]

integrating waste organic carbon utilization, diversifying valuable products, cleaning production, and recycling CO_2 is becoming essential.

Crude glycerol is a primary by-product of the oleochemical industry, such as biodiesel, soap, fatty acid, and fatty ester production [13]. For every 100 tons of biodiesel produced via transesterification, 10 tons of glycerol are produced as the by-product [14, 15]. What is more, glycerol is also produced in the process of bioethanol production, accounting for 7–8% (w/w) of bioethanol [16]. With the mass production of biodiesel and bioethanol, the surplus of crude glycerol results in a low price of pure glycerol, although glycerol is widely used as a chemical in cosmetics, food, solvent, and pharmaceutical industries. For that reason, crude glycerol is considered as an industrial waste production not only because of its low price but also its pollution to the environment [17]. Thus, the conversion of waste glycerol to high value-added products by microbial fermentation is attracting much attention considering the use of a renewable feedstock and environmental performance [18, 19].

Glycerol, as a substrate, could be converted into many value-added chemicals, such as 1,3-propanediol (1,3-PDO), 2,3-butanediol, citric acid, n-butanol, ethanol, lipids, docosahexaenoic acid (DHA), and eicosapentaenoic acid (EPA), using a variety of microorganisms via different metabolic pathways [13, 20–26]. Among these products, 1,3-PDO, an important bulk chemical, is one of the most valuable products. It has been extensively applied in cosmetics, pharmaceuticals, and solvent industries and is especially used for the synthesis of polyester materials, such as polytrimethylene terephthalate (PTT) and polytrimethylene ether glycol [27]. The demand for 1,3-PDO has increased sharply, because PTT has a wide range of applications in the textile industry due to its excellent properties, such as stain resistance, good softness, and low temperature dyeing [28, 29]. The production of 1,3-PDO from glycerol has been extensively investigated using anaerobic or micro-aerobic fermentation with various bacteria, such as *Klebsiella pneumoniae*, *Clostridium butyricum* and *Lactobacillus reuteri* and so on [30–32]. *C. butyricum* is considered as one of the most excellent 1,3-PDO producers due to its superior performance in efficient 1,3-PDO production and less by-products. Meanwhile, it is suitable for industrial production of 1,3-PDO, because it is a probiotic in the intestinal tract and B_{12}-independent bacterium [33]. In the previous report, *C. butyricum* DL07 could produce 104.8 g/L 1,3-PDO from glycerol, and the productivity was up to 3.38 g/L/h in fed-batch fermentation [34], which are among the best results in natural bacteria.

The intracellular metabolic pathway of glycerol in *C. butyricum* has been well-recognized by intracellular metabolic analysis [25]. 1,3-PDO is produced via the metabolic reduction pathway, accompanied by the formation of organic acids, such as butyric acid, acetic acid, and lactic acid in the oxidation branch [35]. Usually, alkaline pH regulators are required to neutralize organic acids and control a constant pH during the fermentation of *C. butyricum*. Otherwise, the organic acids could inhibit 1,3-PDO production, because more energy is needed to maintain the pH in the cell [36, 37]. In general, soluble alkalis such as NaOH, KOH, and ammonia are used to maintain pH (7.0) during fermentation for 1,3-PDO production [32, 38, 39]. However, as the addition of alkalis, the cations such as Na^+, K^+ and NH_4^+ from the alkalis are introduced with high concentration into the fermentation broth, which cause high osmotic pressure and inhibiting the growth of bacterial cells [40]. Furthermore, CO_2 and H_2 are produced in the oxidation branch of glycerol metabolism [41]. The formation of CO_2 not only puts pressure on the environment but also reduces carbon utilization. In addition, the dissolution of CO_2 in fermentation broth would require more alkaline solution to neutralize the fermentation pH. Then, the large amounts of soluble salt in the fermentation broth bring difficulty in the separation of 1,3-PDO. Therefore, the recovery of CO_2 and the reduction of soluble salt concentration in fermentation broth are expected in the microbial production and separation of 1,3-PDO. At the same time, H_2 with a relatively high purity will be available as a clean, sustainable, and ideal energy resource.

Nano- and micro-particles of calcium carbonate ($CaCO_3$), an important material, have been widely used in many fields, such as the construction industry, paper industry, cosmetics, toothpastes, water treatment, pigments, and drug delivery systems [42, 43]. The synthesis of $CaCO_3$ has attracted many researchers' interests in recent years because of its good properties, such as the high ratio of surface area to volume, high porosity, non-toxicity and compatibility toward the human body [44]. $CaCO_3$ can exist in three crystal forms: calcite, vaterite, and aragonite. Calcite is the most stable polymorph and one of the most common minerals on Earth, serving as the main component of sedimentary limestone. At present, calcite ($CaCO_3$) could be synthesized by chemical method and microbially induced precipitation (MIP). MIP is more favored by researchers over chemical synthesis, because it can obtain the controlled single crystal [45]. Regrettably, bacteria-induced $CaCO_3$ usually takes several days and is only produced in small quantities. In a report, *Rhodococcus degradans* BaTD-248 was cultured

for 3 and 21 days to produce $CaCO_3$ [46]. Some ions, such as magnesium, phosphate, citrate, and silicate, as well as the incorporation of amino acid, proteins, extracellular polymeric substance (EPS), and other macromolecules, usually affect bacteria-induced $CaCO_3$ [45–48].

The aim of this study is to propose a novel integrated process for the production of multiple products while avoiding CO_2 emission during fermentation. The optimized process could achieve high-efficient production of 1,3-PDO, high ratio H_2 and micro-nano $CaCO_3$ from industrial waste glycerol by *C. butyricum* DL07. In fed-batch fermentations, NaOH, $Ca(OH)_2$ and double CO_2 capture agents (NaOH & $Ca(OH)_2$) will act as CO_2 capture agents and pH regulators for 1,3-PDO production. The various $Ca(OH)_2$ concentrations and stirring speeds were investigated to produce 1,3-PDO, H_2, and micro-nano $CaCO_3$. Moreover, the effects of this process on the salt concentration, ionic composition and soluble protein concentration in the fermentation broth were discussed.

Results and discussion

Effects of carbon dioxide capture agents on 1,3-PDO production

Efficient 1,3-PDO production using NaOH as a CO_2 capture agent and pH regulator

During the microbial fermentation of 1,3-PDO, organic acids were produced as by-products, as well as CO_2 as exhaust gas, due to redox homeostasis and energy balance during the glycerol metabolism [25, 49, 50]. As a CO_2 capture agent and pH regulator, NaOH was selected to absorb CO_2 and neutralize the organic acids, e.g., 5 M NaOH solution used for anaerobic fermentations by *C. butyricum* DL07. To create anaerobic fermentation environment, nitrogen gas was bubbled into the fermentation medium for 1 h before and after inoculation, respectively, or continuously throughout the whole fermentation process. Regardless of the conditions in the preceding two cases, efficient 1,3-PDO production could be achieved, as shown in Fig. 1a, b. A high 1,3-PDO concentration of

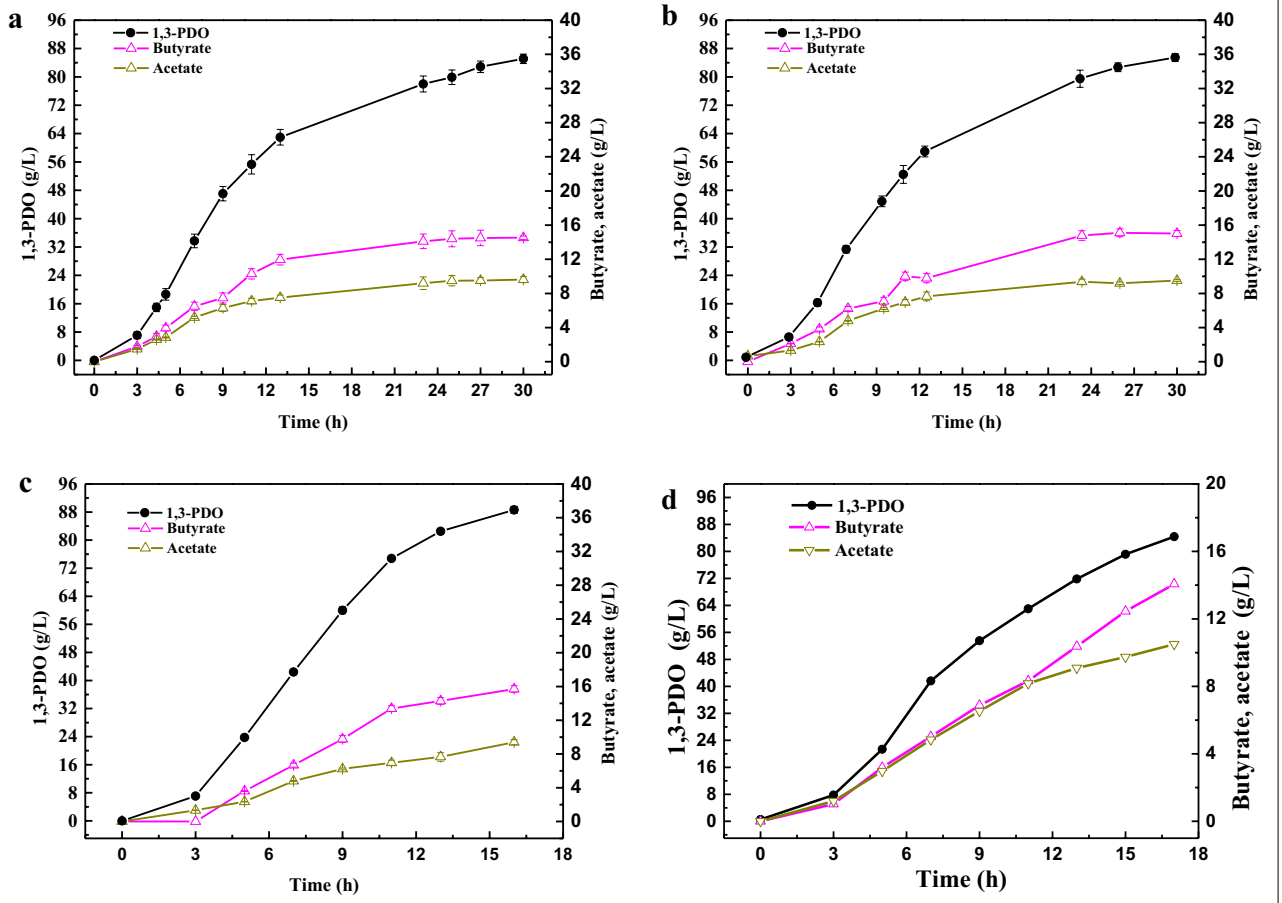

Fig. 1 Profit of products using NaOH (**a**, **b**) or/and $Ca(OH)_2$ (**c**, **d**) as the CO_2 capture agent and pH regulator. 5 M NaOH was employed in **a** and **b**, where **a** was flushed with nitrogen gas for 1 h before and after inoculation and **b** with continuous nitrogen gas flushing throughout the fermentation; 5 M $Ca(OH)_2$ suspension was used in under similar nitrogen gas flushing conditions with **a**; 5 M NaOH and 5 M $Ca(OH)_2$ suspension were used in **d** under similar nitrogen gas flushing conditions with **a**

85.1 g/L was obtained with a satisfying yield of 0.504 g 1,3-PDO/g glycerol and a productivity of 2.84 g/L/h when nitrogen gas was introduced for 1 h before and after inoculation, respectively. Moreover, the concentrations of butyric acid and acetic acid were 14.5 and 9.63 g/L, respectively. While nitrogen gas was continuously pumped into the bioreactor, 1,3-PDO concentration achieved 85.5 g/L with almost the same yield of 0.506 g 1,3-PDO /g glycerol and productivity of 2.85 g/L/h, as well as the concentrations of butyric acid and acetic acid (15.0 and 9.53 g/L, respectively). Fermentations in both of the preceding cases took the same time of 30 h to complete fermentations. Clearly, there was little difference in 1,3-PDO and organic acids production in the above two cases. However, the consumption of 5 M NaOH solution showed significant differences The consumption of 5M NaOH solution was 328 g in the first case, whereas only 241 g 5 M NaOH in the second. This indicates that there were significant differences in the amount of CO_2 captured in the two cases.

C. butyricum IK 124 produced 80.1 g/L of 1,3-PDO with a productivity of 1.80 g/L/h in a fed-batch fermentation using crude glycerol as the substrate [51]. Similar results were obtained, i.e., 80.2 g/L of 1,3-PDO and 1.16 g/L/h of productivity, using *K. pneumoniae* DSM 4799 from crude glycerol [38]. In contrast to previous reported 1,3-PDO production from crude glycerol, *C. butyricum* DL07 could achieve higher concentration (85.0 g/L 1,3-PDO) and productivity (2.84 or 2.85 g/L/h) in this study. When the above two flushing nitrogen gas modes were compared, they had almost no effect on the production of 1,3-PDO and by-products. About 0.340 mol/L organic acids were generated in both fermentation groups. In other words, about 216 g 5 M NaOH solution was required to neutralize the organic acids produced during fermentation, theoretically. However, the theoretical value was less than the actual consumption of 5 M NaOH solution in the first case (328 g) or the second one (241 g), implying that CO_2 fixation levels differed, i.e., 0.24 mol CO_2 fixed in the first case vs. 0.05 mol CO_2 fixed in the second one. This demonstrated that the flushing time of nitrogen gas could affect the fixation of CO_2. Shorter flushing time, more CO_2 would be fixed into Na_2CO_3. Unfortunately, a large amount of Na_2CO_3 in the fermentation broths poses a significant challenge for the separation of 1,3-PDO. Indeed, it is not ignored that a large amount of exhaust gas composed of CO_2 and H_2 from fermentation is discharged into the atmosphere. Therefore, a more significant reduction in CO_2 emissions and soluble salts in the fermentation broth is essential for the industrial fermentation of 1,3-PDO.

High 1,3-PDO productivity using $Ca(OH)_2$ instead of NaOH

To verify the feasibility of 1,3-PDO and other organic acids production using $Ca(OH)_2$ as a CO_2 capture agent and pH regulator, fed-batch fermentations were performed with different concentrations of $Ca(OH)_2$ suspension in comparison to 5 M NaOH solution, as shown in Table 2. In addition, the effect of different stirring speeds (150, 250, 350 rpm) on fermentation was investigated. When 5 M $Ca(OH)_2$ suspension was used, the concentration and productivity of 1,3-PDO were higher, i.e., 85.1 vs. 88.6 g/L and 2.84 vs. 5.54 g/L/h, respectively, when compared to the fermentation using 5 M NaOH, as shown in Fig. 1c and Table 2. As the concentration of $Ca(OH)_2$ suspension decreased, the concentration and productivity of 1,3-PDO were also reduced. For example, only 76.3 g/L 1,3-PDO was produced if $Ca(OH)_2$ concentration decreased to 1.5 M, which is mainly attributed to a dilution effect of low alkaline concentration on fermentation broth. The concentration of butyric acid and acetic acid dropped moderately as a decline of $Ca(OH)_2$ concentration. Unexpectedly, lactic acid was generated using $Ca(OH)_2$ about twice higher than NaOH as listed in Table 2. The above results led to the reduced yield of 1,3-PDO (0.481–0.486 g/g) in $Ca(OH)_2$ group. On the other hand, stirring speed between 150 and 350 rpm had

Table 2 Fed-batch fermentation using different CO_2 capture agent and pH regulator

pH regulator	Fermentation period (h)	1,3-PDO (g/L)	Butyrate (g/L)	Acetate (g/L)	Lactate (g/L)	$Q_{1,3\text{-PDO}}$ (g/L/h)	Yield ($g_{1,3\text{-PDO}}$/g gly)
5M NaOH[a]	30	85.1 ± 1.2	14.5 ± 0.2	9.63 ± 0.1	1.32 ± 0.0	2.84	0.504
5M $Ca(OH)_2$[a]	16	88.6 ± 0.3	15.7 ± 0.1	9.42 ± 0.1	2.91 ± 0.1	5.52	0.486
2.5M $Ca(OH)_2$[a]	16	81.1 ± 1.1	15.0 ± 0.4	8.63 ± 0.1	2.55 ± 0.1	5.14	0.481
1.5M $Ca(OH)_2$[a]	19	76.3 ± 1.3	14.2 ± 0.4	8.15 ± 0.0	2.21 ± 0.0	4.09	0.483
5M $Ca(OH)_2$[b]	16	88.3 ± 0.5	15.8 ± 0.5	9.34 ± 0.2	3.03 ± 0.1	5.51	0.485
5M $Ca(OH)_2$[c]	16	84.5 ± 0.9	15.2 ± 0.4	9.01 ± 0.3	2.82 ± 0.0	5.28	0.483
NaOH & $Ca(OH)_2$[a]	17	84.4 ± 0.6	14.2 ± 0.3	9.81 ± 0.1	1.17 ± 0.0	4.96	0.506

Stirring speed: [a]250 rpm; [b]350 rpm; [c]150 rpm

little effect on fermentation, indicating adequate mixture homogeneity of the fermentation broth obtained at the given stirring speeds and no other effects on microbial metabolism [52].

Up to date, the highest concentration of 1,3-PDO produced by natural producers was 104.8 g/L with a productivity of 3.38 g/L/h, which was achieved in fed-batch fermentation using pure glycerol and a large amount of yeast extract in our previous study [34]. In continuous fermentation, the highest 1,3-PDO productivity was 13.3 g/L/h with a lower 1,3-PDO concentration of 26.5 g/L [53]. The productivity of 1,3-PDO would decrease to 5.55 g/L/h if the 1,3-PDO concentration increased to 57.86 g/L [32]. In this study, the productivity of 1,3-PDO (5.54 g/L/h) obtained in fed-batch fermentation with 5 M $Ca(OH)_2$ suspension was surprisingly 31.9% higher than the previously reported highest level (4.20 g/L/h) of fed-batch fermentation and reached the productivity of continuous fermentation [32, 54]. Moreover, the concentration of 1,3-PDO (88.6 g/L) in fed-batch fermentation was much higher than in continuous fermentation (57.86 g/L) with comparable productivity [32].

It should be emphasized that such high productivity and concentration were achieved in a much shorter fermentation period (16 h) using $Ca(OH)_2$ than NaOH (30 h). A comparison of Fig. 1a, c illustrated that a rapid accumulation of 1,3-PDO occurred from the same start of 8.00 g/L at 3 h to the different end of 64.0 g/L at 13 h in Fig. 1a or 76.1 g/L at 11 h in Fig. 1c, resulting in productivities of 5.60 and 8.51 g/L/h, respectively. In addition, the production trend of 1,3-PDO was not weakened until the end of fermentation in the 5 M $Ca(OH)_2$ group, whereas a significant reduction occurred at the end of fermentation in the 5 M NaOH group. Despite the fact that adding a larger amount of $Ca(OH)_2$ suspension dilutes the fermentation broth, the total 1,3-PDO concentration and productivity achieved in the $Ca(OH)_2$ group were higher than in the NaOH group. This might be due to both Ca^{2+} stimulation on cell growth and a decrease in osmotic pressure, which is relevant to adding $Ca(OH)_2$ during fermentation. Undoubtedly, a high osmotic pressure caused by high soluble salt concentration, e.g., NaOH group, poses a challenge to cell survival and metabolism [55]. The desalination of $Ca(OH)_2$ group will be discussed in Sect. Desalination and deprotein of the fermentation broth. As coupling by-products, butyric acid and acetic acid were found to be positively correlated with the production of 1,3-PDO. The comparative analysis demonstrated that a considerable amount of lactic acid was produced in $Ca(OH)_2$ group compared to the 5 M NaOH group. It was reported that the presence of Ca^{2+} could contribute to the formation of lactic acid [56, 57]. In addition, lactic acid production might be related to citric acid and PO_4^{3-} in the fermentation, which will be discussed in detail in Sect. Desalination and deprotein of the fermentation broth

Although the yield of 1,3-PDO (0.481–0.486 g/g) was reduced in the $Ca(OH)_2$ group, it was comparable to the reported yield of *K. peneumoniae*. For example, a yield of 0.454 g /g with 80.2 g/L 1,3-PDO was obtained by *K. peneumoniae* DSM4799 from crude glycerol [38], and *K. peneumoniae* LX3 obtained a yield of 0.487 g/g accompanied by 71.4 g/L 1,3-PDO using refined glycerol as the substrate [58]. In contrast to *K. peneumoniae*, the production of 1,3-PDO by *C. butyricum* DL07 was still competitive using $Ca(OH)_2$ in the fermentation because of the high concentration of 1,3-PDO (88.6 g/L) with a considerable productivity (5.54 g/L/h) from crude glycerol. Moreover, the CO_2 produced in the fermentation was captured in large quantities, resulting in the insoluble $CaCO_3$ in the fermentation broths. This process is environment-friendly while relieving the pressure of 1,3-PDO separation. Specific details will be discussed later.

Improvement of 1,3-PDO yield using double CO_2 capture agents

A two-stage pH control strategy using double pH regulators has been explored to produce docosahexaenoic acid [59]. The combined application of various CO_2 capture agents was attempted for the production of 1,3-PDO, aiming at increasing the 1,3-PDO yield and reducing the soluble salt concentrations in the fermentation broth. In the first 12 h of fermentation, 5 M NaOH was used to capture CO_2 as well as to regulate the fermentation pH, and then 5 M $Ca(OH)_2$ suspension instead of 5 M NaOH was employed to proceed with the fermentation. The results showed that the concentration of 1,3-PDO was 84.4 g/L in 17 h, accompanied by a productivity of 4.96 g/L/h (Fig. 1d). More importantly, the yield of 1,3-PDO reached 0.506 g 1,3-PDO /g glycerol, which was equal to that of the 5 M NaOH group. It is reported that the maximum theoretical 1,3-PDO yield is 0.72 mol 1,3-PDO/mol glycerol (about 0.60 g 1,3-PDO/g glycerol), which is calculated by kinetic analysis of *C. butyricum* based on no formation of hydrogen and butyric acid [60]. Regardless of CO_2 capture agent and pH regulator (NaOH, $Ca(OH)_2$ or NaOH & $Ca(OH)_2$), *C. butyricum* DL07 could produce up to 84.4–88.6 g/L 1,3-PDO with the yield of 0.481–0.506 g 1,3-PDO/g glycerol. Moreover, the 1,3-PDO productivity was about 2.84–5.54 g/L/h. These values indicated that *C. butyricum* DL07 had excellent 1,3-PDO production performance according to 1,3-PDO production using different pH regulators in some recent reports (Table 3). Double CO_2 capture agents prevented the reduction of yield of 1,3-PDO in the $Ca(OH)_2$

Table 3 1,3-PDO production by natural 1,3-PDO producers from glycerol in fed-batch fermentation

Microorganism	Titer (g/L)	Yield (g/g)	Overall productivity (g/L/h)	pH regulator	Refs.
K. pneumoniae HSL4	80.1	0.44	2.22	NaOH	[61]
K. pneumoniae LX3	71.4	0.49	2.24	NaOH	[58]
K. pneumoniae KXJPD-Li	65.3	0.46	1.36	KOH	[62]
C. butyricum VPI 1718	67.9	0.55	0.78	NaOH	[35]
C. butyricum AKR 102	50.5	0.47	1.80	NaOH	[28]
C. butyricum SCUT343-4	59.2	0.53	2.11	NaOH	[54]
C. butyricum (Gen 7)	66.2	0.51	1.38	NaOH	[63]
C. pasteurianum	81.2	0.49	4.27	Ammonia	[64]
C. freundii FMCC-B294	68.1	0.40	0.79	NaOH	[65]
C. freundii VK19	47.2	0.38	0.73	NaOH	[66]
[a]*L. reuteri* DSM 20016	52.3	0.51	1.09	Ammonia	[67]
Mixed culture	70.0	0.56	2.60	NaOH	[68]
Microbial consortium C2-2 M	82.7	0.54	3.06	NaOH	[69]
Microbial consortium CJD-S	41.5	0.34	1.15	NaOH	[70]
C. butyricum DL07	85.1	0.50	2.84	NaOH	This study
	88.6	0.49	5.54	$Ca(OH)_2$	
	84.4	0.51	4.96	NaOH & $Ca(OH)_2$	

[a] Glycerol and xylose as co-substrate

group, while butyric acid (14.2 g/L) and acetic acid (9.81 g/L) showed negligible changes. The production of lactic acid was only 1.17 g/L, which was similar to that of NaOH group, but greatly different from the $Ca(OH)_2$ group (Additional file 1: Fig. S1). Little difference in the production of lactic acid within 5 h of the fermentation occurred in the three groups. However, after 5 h of fermentation, lactic acid concentration continued to rise in the $Ca(OH)_2$ group, but remained almost unchanged in both the NaOH group and the double alkalis group (NaOH & $Ca(OH)_2$).

In the process of converting glycerol to 1,3-PDO by *C. butyricum* DL07, when $Ca(OH)_2$ was the only CO_2 capture agent and pH regulator, the productivity of 1,3-PDO was greatly improved. Regrettably, the yield of 1,3-PDO has decreased. A process with satisfactory 1,3-PDO yield, productivity and concentration is expected to reduce 1,3-PDO production costs. Fortunately, using double CO_2 capture agents resulted in an increase in 1,3-PDO yield (0.506 g/g) with satisfactory 1,3-PDO concentration (84.4 g/L) and productivity (4.96 g/L/h). Furthermore, the production of lactic acid showed the same trend (almost constant concentration from 5 h to the end point of fermentation) in the double CO_2 capture agents group as compared to the NaOH group, whereas more lactic acid was produced after 5 h of fermentation in $Ca(OH)_2$ group (Additional file 1: Fig. S1). A large amount of Ca^{2+} has been reported to contribute to the formation of lactic acid [56, 57]. It can be inferred that the presence of a large amount of Ca^{2+} at the early stage of fermentation could activate metabolic pathways of lactic acid, resulting in a continuous increase of lactic acid production until the end of fermentation and a further reduction in 1,3-PDO yield (Additional file 1: Fig. S1). When NaOH was used rather than $Ca(OH)_2$ in the early fermentation stage, that is, there is little Ca^{2+} in the early fermentation stage, and lactic acid was not produced in large quantities. As a result, the 1,3-PDO yield was improved using double CO_2 capture agents. It is a promising process to employ double CO_2 capture agents and pH regulators in fermentation to achieve high concentration, yield, and productivity of 1,3-PDO.

In situ carbon dioxide capture to form micro-nano calcium carbonate

H_2 and CO_2 as exhaust gases are produced in glycerol metabolism by *C. butyricum*. In fermentation, $Ca(OH)_2$ acts as a CO_2 capture agent allowing for cleaner production and the synthesis of valuable products. In theory, $CaCO_3$ could be generated in fermentation once $Ca(OH)_2$ reacts with CO_2. The concentration of $Ca(OH)_2$ suspension and the stirring speed of fermentation have a non-negligible effect on the size of $CaCO_3$ particles [44]. As a result, the production of $CaCO_3$ was investigated using various $Ca(OH)_2$ concentrations and fermentation stirring speeds (Fig. 2). When 5 M $Ca(OH)_2$ suspension was used as a CO_2 capture agent at the stirring speed of

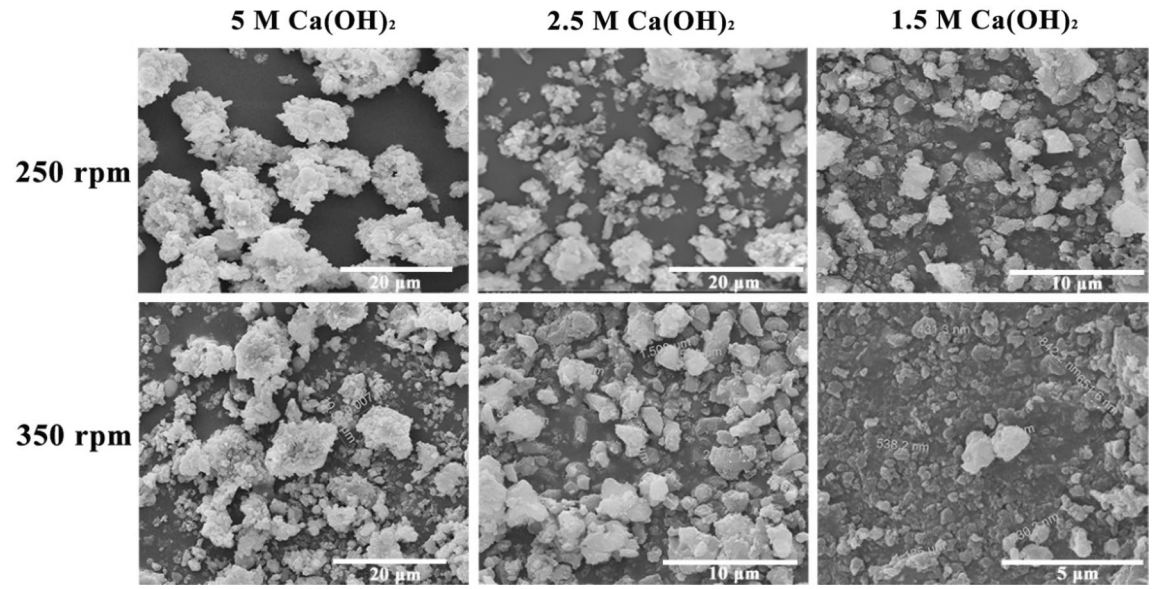

Fig. 2 SEM images of precipitations produced during fermentation at different $Ca(OH)_2$ concentrations and stirring speeds

250 rpm, the highest amount of precipitate (76.8 g/L) was obtained in fermentation. The precipitates showed a decreasing trend as the $Ca(OH)_2$ concentration was reduced. Subsequently, the precipitations collected from fermentations were observed by SEM. Most particles with a size of 10–15 μm were produced using 5 M $Ca(OH)_2$ suspension and the stirring speed of 250 rpm. When the concentration of $Ca(OH)_2$ suspension was reduced to 2.5 M, a large proportion of particles were distributed between 5 and 10 μm. Using 1.5 M $Ca(OH)_2$ suspension as the CO_2 capture agent, particles with a large size limit of 5 μm were obtained. In addition, by increasing the fermentation stirring speed to 350 rpm, further small-size precipitations were observed. Precipitations in fermentation were smaller than 5 μm in the 2.5 M $Ca(OH)_2$ group. Surprisingly, the nano-particles were produced using 1.5 M $Ca(OH)_2$ suspension. The precipitations were not completely individual particles, according to the SEM images, but a portion of them were aggregated.

Elemental composition analysis was performed by energy dispersive X-ray spectroscopy (EDX) at 15.0 keV to identify the elemental compositions in the precipitations. The EDX spectra for the precipitations in 5 M $Ca(OH)_2$ group was presented in Fig. 3. Moreover, the EDX analysis of commercial pure $CaCO_3$ was also conducted to serve as standard sample. As a result, calcium, carbon, and oxygen as the most abundant elements were determined in precipitations collected in the fermentation. Further comparison with the EDX spectra of pure $CaCO_3$, revealed a high degree of similarity in the EDX spectra between these precipitations and pure $CaCO_3$. it can be concluded that the precipitations produced during fermentation were $CaCO_3$ particles. Finally, the crystal form of $CaCO_3$ particles was characterized by XRD. As indicated by XRD spectra (Additional file 1: Fig. S2), the intensive peaks of the sample exhibited high agreement with the standard spectrum (Calcite CaCO3: PDF#86-2334), demonstrating that the generated $CaCO_3$ particles existed in calcite crystal.

It has been reported that many microorganisms, including *Bacillus pasteurii, Bacillus mucilaginosus, Bacillus alcalophilus, Photosynthetic bacteria* could induce $CaCO_3$ formation except *C. butyricum* [46, 71, 72]. The CO_2 released by *C. butyricum* could undoubtedly react with $Ca(OH)_2$, resulting in the formation of $CaCO_3$. The precipitations of various sizes in the fermentation were observed by a SEM, while the concentration of $Ca(OH)_2$ and the stirring speed of the fermentation were changed. Obviously, the size of $CaCO_3$ particles formed in fermentation decreased as the concentration of $Ca(OH)_2$ suspension decreased and the stirring speed of fermentation increased. After all, the stirring speed can affect the precipitation crystal and size [73, 74]. The synthesis of micro-particles was accomplished under 2.5–5 M $Ca(OH)_2$ suspension with 250–350 rpm stirring speed as well as 1.5M $Ca(OH)_2$ suspension with 250 rpm stirring speed. The nano-particles were synthesized using the 1.5 M $Ca(OH)_2$ suspension and a stirring speed of 350 rpm. Therefore, it can be concluded that micro/

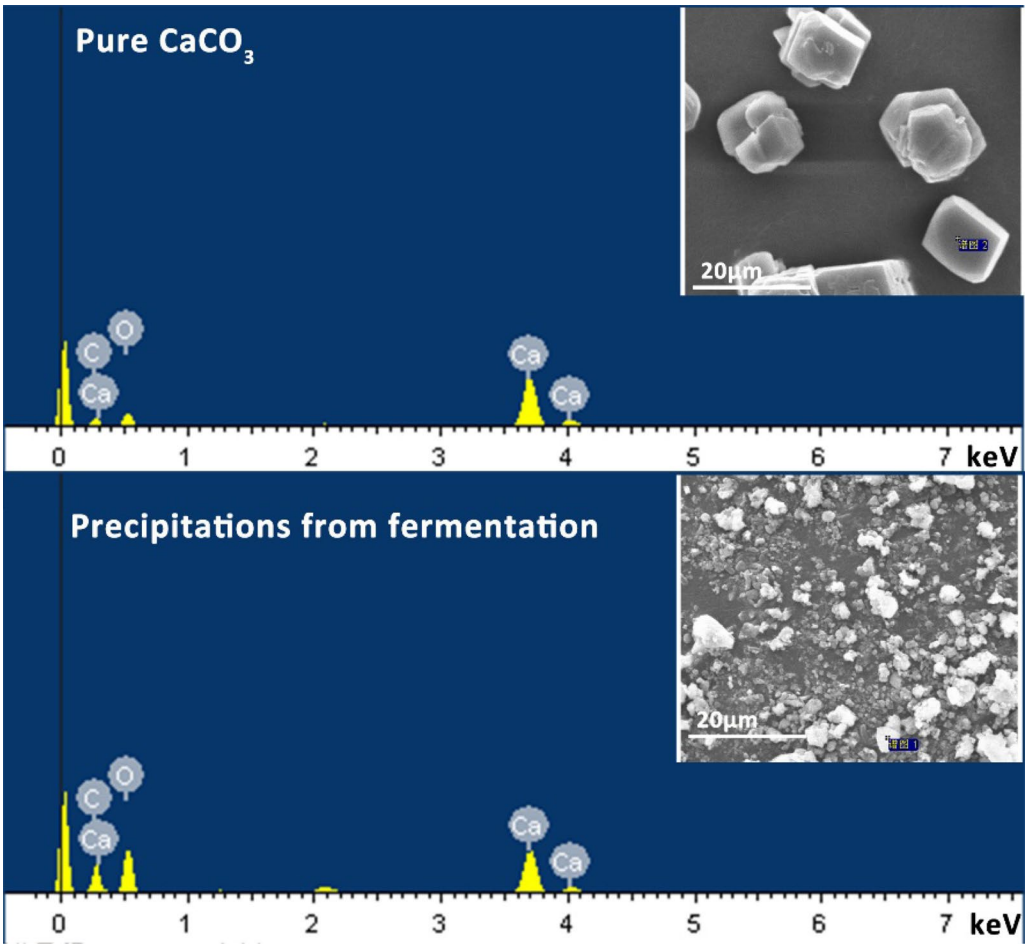

Fig. 3 EDS and SEM images of pure $CaCO_3$ and precipitations collected in the fermentation

nano $CaCO_3$ was produced as calcite during the production of 1,3-PDO by *C. butyricum* DL07. Bacteria could induce various crystalline $CaCO_3$ in the form of calcite, aragonite, vaterite and amorphous $CaCO_3$. In general, the effects of induction conditions and time on the crystal form and size of $CaCO_3$ are investigated using microbial induction method, but the productivity of $CaCO_3$ is rarely reported. Magnesium, potassium, phosphate, citric acid, amino acids, polysaccharides, and proteins have all been linked to the formation of $CaCO_3$ crystals [45–48]. It can be considered that the formation of calcite was related to the presence of magnesium, potassium, phosphate, citric acid, glycerol and so on in fermentation broth, and even to the polysaccharides and proteins produced by *C. butyricum* DL07. A complex process resulted in the production of stable calcite ($CaCO_3$), allowing CO_2 to be converted into high value products during the fermentation. Although calcite is the most common crystalline form, the time required to form $CaCO_3$ was reduced from more than 3 days reported by microbial induced method to 16 h using glycerol fermentation [46]. To our knowledge, micro-nano $CaCO_3$ and *C. butyricum* could be obtained separately by differential centrifugation after fermentation because of their different sedimentation coefficients. Calcite $CaCO_3$ could be widely applied in the construction industry. Moreover, a popular mixture of $CaCO_3$ and living probiotics can be widely used as animal feed.

Improved ratio of hydrogen in the exhaust gas

In general, a mixture of H_2 and CO_2 as exhaust gas was released from most microbial fermentations into the environment [75, 76]. Based on $Ca(OH)_2$ as CO_2 capture agent, the composition of exhaust gas was detected and expressed as percentage difference (Fig. 4), with 5 M NaOH as the control. At the end of fermentation, the ratio of H_2 to CO_2 in exhaust gas was 0.0659 in the NaOH group, accounting for a CO_2 composition of 92.4%

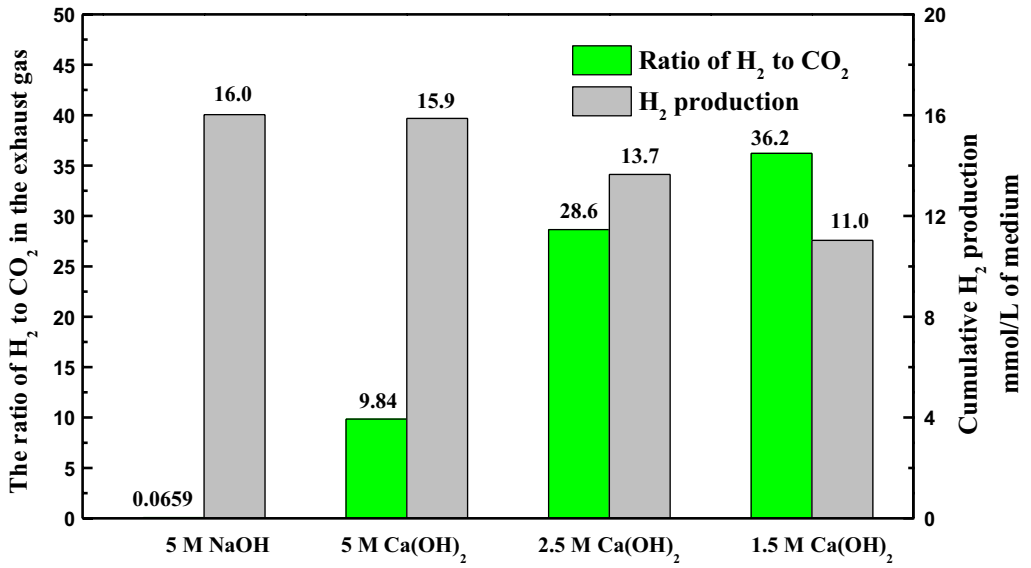

Fig. 4 Ratio of H_2 to CO_2 and H_2 production in the fermentation with different concentrations of CO_2 capture agent

along with 6.09% H_2 (Additional file 1: Fig. S3). When $Ca(OH)_2$ was selected as a CO_2 capture agent, the ratio of H_2 to CO_2 increased significantly, i.e., 9.84 with a H_2 proportion of 17.2% in the 5 M $Ca(OH)_2$ group, 28.6 in the 2.5 M $Ca(OH)_2$ group, and 36.2 in the 1.5 M $Ca(OH)_2$ group. Regrettably, in the double CO_2 capture agents group, the ratio of H_2 to CO_2 was reduced to 0.203, with a H_2 proportion of 9.21% and CO_2 proportion of 45.3% in exhaust gas. The highest H_2 production of 15.9 mmol/L of medium was achieved using 5 M $Ca(OH)_2$ suspension and 11.0 mmol/L of medium as the lowest concentration was produced with 1.5 M $Ca(OH)_2$ suspension as the CO_2 capture agent.

C. butyricum is commonly employed to produce H_2 [77]. The ratio of H_2 to CO_2 in exhaust gas of fermentation would increase if CO_2 was captured, which will contribute to the separation of H_2. Expectedly, the proportion of CO_2 significantly decreased, because CO_2 was converted into $CaCO_3$ particles in the fermentation. Indeed, there was a significant reduction in the proportion of CO_2 (< 1.75%) in the 5 M $Ca(OH)_2$ group. The results showed that the ratio of H_2 to CO_2 was 152 times higher in the 5 M $Ca(OH)_2$ group than the 5 M NaOH group indicating that $Ca(OH)_2$ had a more outstanding CO_2 fixation level. As the $Ca(OH)_2$ concentration decreased, the production of H_2 and CO_2 was declined, but has led to a rising ratio of H_2 to CO_2 (Fig. 4 and Additional file 1: Fig. S3). This indicated that a reduced productivity of CO_2 in fermentation caused by lower $Ca(OH)_2$ concentration made $Ca(OH)_2$ to fix CO_2 more efficiently. Thus, the proportion of CO_2 in the exhaust gas decreased as $Ca(OH)_2$ concentration decreased, and the value was almost close to zero. On the contrary, the proportion of H_2 in the exhaust gas increased slightly as $Ca(OH)_2$ concentration decreased. Therefore, the H_2/CO_2 ratio decreased with $Ca(OH)_2$ concentration significantly. Apparently, the ratio of H_2 to CO_2 in the double CO_2 capture agents group (0.203) had a significant decrease compared to the $Ca(OH)_2$ group due to the poor CO_2 capture agent (NaOH) acting in the first 12 h of the fermentation. There is no doubt that more CO_2 would be fixed to form $CaCO_3$ in situ as long as the excellent CO_2 capture agent ($Ca(OH)_2$) was employed as soon as possible in the fermentation, surely obtaining a higher ratio of H_2 to CO_2. Therefore, it can be concluded that the earlier $Ca(OH)_2$ is introduced into fermentation, the higher H_2 ratio with lower CO_2 ratio appears in the exhaust gas. In the future, the addition time of $Ca(OH)_2$ should be optimized for a higher ratio of H_2 to CO_2 in double CO_2 capture agents. The accumulated H_2 production ranged between 11.0 and 15.9 mmol/L of medium, which was in agreement with the previous reported [78]. H_2 production decreased as $Ca(OH)_2$ concentration decreased, following the same trend as the production of 1,3-PDO, owing to a dilution effect of $Ca(OH)_2$ suspension. Studies on microbial fermentation accompanied by in situ CO_2 capture are rarely reported. Many studies had reported biohydrogen production using *C. butyricum*,

but only focusing on the total hydrogen production, not on the ratio of H_2 in the exhaust [78–81]. Actually, the ratio of H_2 to CO_2 is concerned with the separation of H_2, since normally CO_2 plays an indispensable role in most microbial fermentation [49]. This new process proposed in this study provides a reference for microbial fermentation to capture CO_2 and improves the ratio of H_2 in the exhaust gas in the future.

Desalination and deprotein of the fermentation broth

The higher salt concentration in the fermentation broth could affect 1,3-PDO fermentation efficiency, because the high osmotic pressure caused by a large amount of soluble salts poses a challenge to cell survival [82]. More importantly, the high salt concentration can complicate the product separation process [83]. CO_3^{2+} was present in the fermentation broth, as CO_2 produced by microbial metabolism dissolved in water. As a result, once $Ca(OH)_2$ was selected as the CO_2 capture agent rather than NaOH, insoluble $CaCO_3$ instead of soluble Na_2CO_3 would present in the fermentation broth. To further reduce soluble salts in the fermentation broths, quantitative ammonium hydroxide as a pH regulator was added after fermentation initiation to substitute ammonium sulfate of the fermentation media as an inorganic nitrogen source without affecting the 1,3-PDO concentration (Additional file 1: Fig. S4). As expected, differences in conductivity values were observed under different fermentation conditions (Fig. 5). The highest conductivity value of fermentation broth (42,665 μs/cm) was present in the control group (5 M NaOH group). Conversely, the ammonium hydroxide and the 5 M $Ca(OH)_2$ group had the lowest conductivity values (19,800 μs/cm). Thus, the salt concentration of the fermentation broth was reduced by 53.6%. The fermentation broth showed a relatively low conductivity when ammonium hydroxide replaced ammonium sulfate of the fermentation media, mainly due to reduced sulfate. Apparently, when $Ca(OH)_2$ was added into the fermentation, the conductivity values rose slowly during the subsequent fermentation, indicating the production of insoluble salts. It demonstrated that the addition of $Ca(OH)_2$ can effectively reduce the soluble salt concentrations of the fermentation broth, thereby contributing to the separation of 1,3-PDO. In addition, the productivity and concentration of 1,3-PDO in $Ca(OH)_2$ group were significantly higher than in NaOH group. It is quite possible that the formation of insoluble $CaCO_3$ would result in lower osmotic pressure of fermentation broth, which leads to a lower osmotic pressure for cell, which is beneficial for cell survival and 1,3-PDO production.

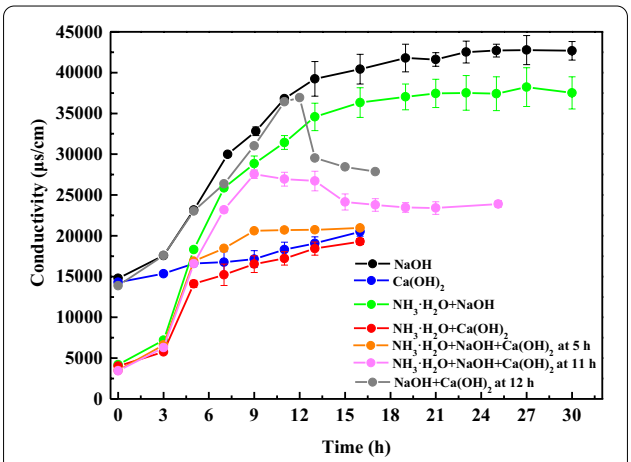

Fig. 5 Conductivities of fermentation broths under different CO_2 capture scenarios. NaOH represents 5 M NaOH solution; $Ca(OH)_2$ represents 5 M $Ca(OH)_2$ suspension; In the ammonium hydroxide group, ammonium hydroxide acted as an inorganic nitrogen source and, otherwise, $(NH_4)_2SO_4$ acted as an inorganic nitrogen source

For using double CO_2 capture agents, when 5 M $Ca(OH)_2$ suspension was introduced in fermentation at 5 h, the conductivity value of the fermentation broth was 20,960 μs/cm, whereas when $Ca(OH)_2$ was involved in fermentation from 11 h, the conductivity was 23,900 μs/cm. Thus, the earlier $Ca(OH)_2$ was involved in fermentation, the less soluble salts were present in the fermentation broth. To further clarify the main ion species and specific concentration existed in the fermentation broths, concentration of ions was determined at the end of fermentation. The results showed that large differences in concentration were exhibited in some ions (SO_4^{2}, PO_4^{3-}, Na^+, Ca^{2+}) during the fermentation with different CO_2 capture agents (Table 4). Compared to the 5 M NaOH group (13,043.60 mg/L), the concentration of Na^+ of fermentation broth was reduced by 99.7% in the 5 M $Ca(OH)_2$ group (38.61 mg/L). Conversely, Ca^{2+} concentration was increased from 64.74 mg/L to 6308.75 mg/L. When $Ca(OH)_2$ participated in the fermentation, there

Table 4 Ions concentration of fermentation broth using different CO_2 capture agents and pH regulators

Ions (mg/L)	A	B	C	D
Cl^-	221.65	169.50	190.40	171.42
SO_4^{2-}	3268.58	539.96	14.28	3.57
PO_4^{3-}	423.68	0.00	403.42	0.00
Na^+	13,043.60	38.61	10,865.96	47.55
K^+	453.91	446.88	454.60	451.85
NH_4^+	0.00	0.00	3.62	5.91
Ca^{2+}	64.74	6308.75	90.00	5658.55

A and C represent 5 M NaOH as the CO_2 capture agent and pH regulator; B and D represent 5 M $Ca(OH)_2$ as the CO_2 capture agent and pH regulator; $(NH_4)_2SO_4$ was supplemented into the medium of A and C; Ammonium hydroxide was added in B and D group during the fermentation

was no PO_4^{3-} in the fermentation broth. This indicated that $Ca_3(PO_4)_2$ precipitations existed in the fermentation broth. At the same time, regardless of the fermentation conditions, the NH_4^+ added to the media was almost absent at the end of the fermentation, which should be attributed to the microbial uptake. There was little difference in the concentration of Cl^- and K^+ concentrations, although different CO_2 capture agents were used in the fermentation. Overall, the total ion concentration in $Ca(OH)_2$ group was about half that of the NaOH group.

Surprisingly, there were also significant differences in soluble protein concentration of fermentation broth when 5 M $Ca(OH)_2$ suspension and 5 M NaOH were selected as the CO_2 capture agent and pH regulator, respectively. The soluble protein concentration of 5M $Ca(OH)_2$ group was only 1.52 g/L, while that of the 5 M NaOH group was up to 2.72 g/L. This result suggested that the soluble proteins of the fermentation broth decreased by 44.1% with 5 M $Ca(OH)_2$ suspension as the CO_2 capture agent and pH regulator when compared to 5 M NaOH. It is speculated that the reduced salt concentrations in fermentation broth caused by insoluble $CaCO_3$ pose fewer threats to cells, allowing for the avoidance of proteins synthesis and bacterial cell lyses. After all, high osmotic stress imposes pressure on bacteria to synthesize multiple characteristic proteins, such as membrane proteins and translocators [84], and it may even regulate bacterial death to release intracellular proteins [85]. Lower soluble salt and protein concentrations can effectively facilitate the separation of 1,3-PDO while alleviating the wastewater treatment problem, thereby contributing to sustainable development goals.

Conclusions

Higher concentrations of 1,3-PDO (>80.0 g/L) were accomplished from waste crude glycerol by *C. butyricum* DL07 either using NaOH, $Ca(OH)_2$ or both combinations as the CO_2 capture agent and pH regulator. The highest 1,3-PDO concentration (88.6 g/L) accompanied by the highest reported productivity (5.54 g/L/h) was achieved, while 5 M $Ca(OH)_2$ suspension acted as the CO_2 capture agent in fed-batch fermentation. Simultaneously, CO_2 was captured in situ to produce $CaCO_3$ and improve the ratio of H_2 to CO_2 in the exhaust gas. Furthermore, the $CaCO_3$ produced during fermentation existed in calcite, and its size gradually decreased as the concentration of the $Ca(OH)_2$ suspension decreased and fermentation speed increased. Nano-$CaCO_3$ was synthesized in 1.5 M $Ca(OH)_2$ group with a stirring speed of 350 rpm. More importantly, the produced CO_2 by waste crude glycerol fermentation was almost entirely captured in situ, which resulted in a 152-fold increase in the ratio of H_2 to CO_2. In this process, the conductivity of the fermentation broth was reduced significantly in $Ca(OH)_2$ group because of the generation of insoluble $CaCO_3$. When ammonium hydroxide was added in the 5 M $Ca(OH)_2$ group as an inorganic nitrogen source instead of $(NH_4)_2SO_4$, the conductivity of the fermentation broth was reduced by 54.3% when compared to the 5 M NaOH group. The soluble protein concentration of fermentation broth was obviously decreased by 44.1%, while 5 M $Ca(OH)_2$ suspension was employed as the CO_2 capture agent and pH regulator rather than 5 M NaOH. The reduced soluble salt and protein concentrations in the fermentation broth will significantly contribute to the downstream product separation process. Undoubtedly, the pressure of wastewater treatment would also be relieved, promoting the green production process. This new process integrates the generation of important chemicals (1,3-PDO), material ($CaCO_3$) and clean energy (H_2) using waste glycerol with a dramatically reduced carbon footprint. Therefore, this process provides a green and environmentally friendly production method for 1,3-PDO, which is highly consistent with sustainable development goals and serves as a valid reference for the production of bio-based chemicals to achieve net-zero CO_2 emissions. It will broaden the range of applications for bio-based chemicals.

Methods

Microorganism and culture media

C. butyricum DL07, previously selected from anaerobic active sludge [34], was used in this study. It was stored at − 70 °C using a seed medium with 40% glycerol in the lab as well as China General Microbiological Culture Collection Center (CGMCC NO. 17934). The seed and fermentation media were prepared as described in our previous work [34], but ammonium sulfate was not added to the fermentation medium when ammonia was involved in controlling the fermentation pH. Crude glycerol was used as substrate in seed and fermentation media. 100 mL of seed medium was fed into 250 mL anaerobic serum bottles and bubbled with nitrogen gas. The seed and fermentation media were sterilized at 121 °C for 20 min. Crude glycerol was supplied from Sichuan Tianyu Oleochemical Co. Ltd., China. Its components had been described in previous study [69].

Culture conditions

C. butyricum DL07 was revived and cultured in seed medium. 4% (v/v) of strain suspension was inoculated into the seed medium. The seed culture was carried out in shaker at 37 °C and 200 rpm for 12 h. Fermentations were performed in a 5.0 L bioreactor (Baoxing Biotech,

Shanghai, China) containing 2.0 L fermentation medium. To ensure an anaerobic environment, N_2 was bubbled into the fermentation medium at 0.15 vvm, starting at 1 h before inoculation, and then stopped at 1 h after inoculation. 10% (v/v) of inoculum was inoculated into the bioreactor. The bioreactor was automatically run at various stirring speeds according to the experimental design. Throughout the fermentation process, the pH was maintained by different concentrations of $Ca(OH)_2$ suspension involving NaOH and ammonia (6.80 g/L). $Ca(OH)_2$ suspension was stirred at 100 rpm during service period.

Fed-batch fermentations for the co-production 1,3-PDO, $CaCO_3$ and H_2

Fed-batch fermentations were carried out using continuous feeding strategy. The initial glycerol concentration was 40 g/L. When the residual glycerol concentration dropped to 20 g/L, crude glycerol was manually pumped into the bioreactor to maintain the glycerol concentration of about 20 g/L during the fermentation. The detailed operation of fermentation can refer to the previous report [34]. The exhaust gas produced in the bioreactor was collected manually using a 1 L gas collection bag. All $CaCO_3$ deposits were collected by centrifugation at 5000 rpm for 10 min.

Analytical methods

Cell mass was represented by the optical density of the sample at 650 nm using a UV–visible spectroscopy system (UV-5100, Metash Instruments Co. Ltd, Shanghai, China). The concentrations of 1,3-PDO, glycerol and acids (butyric acid, acetic acid and lactic acid) were analyzed by high performance liquid chromatography (Waters, Milford, USA) equipped with an Aminex HPX 87H column (300 × 7.8 mm) (Bio-Rad, Hercules, CA), a differential refractometer (Waters 2414) and an autosampler (Waters 2707). Operating conditions applied for detector temperatures, column temperature, the flow rate of mobile phase (5 mM H_2SO_4) and sample volume were 35 °C, 65 °C, 0.6 mL/min and 20 μL, respectively. Each testing sample from the fermentation broths was centrifuged for 10 min at 12,000 r/min. The clarified fermentation broth and chloroform were mixed at a ratio of 1:1 and centrifuged again under the above conditions to remove soluble proteins. After proper dilution, the above sample was filtered through a 0.22 μm membrane filter for analysis. All the precipitates were washed twice with pure water to remove impurities before being dried at 50 °C until constant weight for the collection of $CaCO_3$. The collected exhaust gas was detected by gas chromatography (GC-7900, Techcomp Co., Ltd. Shanghai, China). The conductivity of fermentation broth was measured using an intelligent conductivity meter. The ions in the fermentation broth were analyzed using high-performance ion chromatography. The concentration of soluble proteins contained in the fermentation broth was determined by the bradford protein assay kit (Beyotime Biotech, Shanghai, China).

The fixed CO_2 (mol) in the fermentation was calculated according to the following formula. Where consumption of NaOH is the consumption of NaOH in the fermentation. Total organic acids are the total organic acids produced in the fermentation.

$$\begin{aligned}\text{Fixed } CO_2\text{(mol)} &= \text{Consumption of NaOH (mol)} \\ &\quad - \text{Total organic acids (mol)}\end{aligned}$$

$CaCO_3$ particles characterization

The elemental composition of precipitations was analyzed by energy dispersive spectrometer (EDS) equipped with an SEM instrument. The morphology of $CaCO_3$ was examined by a scanning electron microscopy (SEM; FEI Quanta 450, The USA). The polymorphs of $CaCO_3$ particles were characterized via X-ray diffraction (XRD) with Rigaku D/max 2400 V diffractometer (Japan).

Abbreviations

1,3-PDO: 1,3-Propanediol; LCA: Life cycle assessment; TCA: Techno-economic assessment; DHA: Docosahexaenoic acid; EPA: Eicosapentaenoic acid; PTT: Polytrimethylene terephthalate; MIP: Microbially induced precipitation; EPS: Extracellular polymeric substance. EDX: energy dispersive X-ray spectroscopy; SEM: Scanning electron microscopy.

Supplementary Information

The online version contains supplementary material available at https://doi.org/10.1186/s13068-022-02190-2.

Additional file 1: **Fig. S1** Production of lactic acid using different CO_2 capture agents. The solid symbol represents lactic acid production, and the hollow symbol represents citric acid consumption. The stirring speed is 250 rpm in every groups. **Fig. S2** XRD pattern of $CaCO_3$ from the fermentation. **Fig. S3** Ratio of H_2 and CO_2 in exhaust gas using different CO_2 capture strategies. **Fig. S4** 1,3-PDO production under different CO_2 capture scenarios. NaOH represents 5 M NaOH solution; $Ca(OH)_2$ represents 5 M $Ca(OH)_2$ solution; In the ammonium hydroxide group, ammonium hydroxide acted as an inorganic nitrogen source and, otherwise, $(NH_4)_2SO_4$ acted as an inorganic nitrogen source.

Acknowledgements

Not applicable.

Author contributions

Z-LX and X-LW contributed conception and design of the study. X-LW performed the experiments with the assistance of SL. X-LW, J-JZ and Y-QS analyzed and discussed the data. X-LW wrote the original manuscript. All authors contributed to manuscript revision, read, and approved the submitted version. All authors read and approved the final manuscript.

Funding
This work was supported by the National Natural Science Foundation of China (Grant No. 21476042, awarded to Zhi-Long Xiu).

Availability of data and materials
The data sets supporting the results reported in this article are included within the article and its Additional files.

Declarations

Ethics approval and consent to participate
Not applicable.

Consent for publication
Not applicable.

Competing interests
The authors declare no conflict of interest.

Received: 18 January 2022 Accepted: 26 August 2022
Published online: 03 September 2022

References

1. Petit JR, Jouzel J, Raynaud D, Barkov NI, Barnola JM, Basile I, Bender M, Chappellaz J, Davis M, Delaygue G, Delmotte M, Kotlyakov VM, Legrand M, Lipenkov VY, Lorius C, Pépin L, Ritz C, Saltzman E, Stievenard M. Climate and atmospheric history of the past 420,000 years from the Vostok ice core. Antarctica Nature. 1999;399:429–36.
2. Earth's CO_2 Home Page. https://www.co2.earth/. Accessed July 2021.
3. Liu Z, Wang K, Chen Y, Tan Tand Nielsen J. Third-generation biorefineries as the means to produce fuels and chemicals from CO_2. Nat Catal. 2020;3:274–88.
4. Wang T, Jiang Z, Zhao B, Gu Y, Liou K, Kalandiyur N, Zhang D, Zhu Y. Health co-benefits of achieving sustainable net-zero greenhouse gas emissions in California. Nat Sustain. 2020;3:597–605.
5. Ögmundarson Ó, Sukumara S, Herrgård MJ, Fantke P. Combining environmental and economic performance for bioprocess optimization. Trends Biotechnol. 2020;38:1203–14.
6. Wyman CE, Hinman ND. Ethanol. Appl Biochem. Biotech. 1990;24:735–53.
7. Lee SY, Kim HU, Chae TU, Cho JS, Kim JW, Shin JH, Kim DI, Ko Y, Jang WD, Jang Y. A comprehensive metabolic map for production of bio-based chemicals. Nat Catal. 2019;2:18–33.
8. Nakamura CE, Whited GM. Metabolic engineering for the microbial production of 1,3-propanediol. Curr Opin Biotech. 2003;14:454–9.
9. Burgard A, Burk MJ, Osterhout R, Van Dien S, Yim H. Development of a commercial scale process for production of 1,4-butanediol from sugar. Curr Opin Biotech. 2016;42:118–25.
10. Waltz E. Cathay Industrial Biotech: this Chinese biotech exemplifies how companies in emerging markets can thrive in low-margin industrial application. Nat Biotechnol. 2012;30:480.
11. Veza I, Muhamad Said MF, Latiff ZA. Recent advances in butanol production by acetone-butanol-ethanol (ABE) fermentation. Biomass Bioenergy. 2021;144: 105919.
12. Ögmundarson Ó, Herrgård MJ, Forster J, Hauschild MZ, Fantke P. Addressing environmental sustainability of biochemicals. Nat Sustain. 2020;3:167–74.
13. Clomburg JM, Gonzalez R. Anaerobic fermentation of glycerol: a platform for renewable fuels and chemicals. Trends Biotechnol. 2013;31:20–8.
14. Luo X, Ge X, Cui S, Li Y. Value-added processing of crude glycerol into chemicals and polymers. Bioresource Technol. 2016;215:144–54.
15. Amorim HV, Lopes ML, de Castro Oliveira JV, Buckeridge MS, Goldman GH. Scientific challenges of bioethanol production in Brazil. Appl Microbiol Biotechnol. 2011;91:1267–75.
16. Westbrook AW, Miscevic D, Kilpatrick S, Bruder MR, Moo-Young M, Chou CP. Strain engineering for microbial production of value-added chemicals and fuels from glycerol. Biotechnol Adv. 2019;37:538–68.
17. Russmayer H, Egermeier M, Kalemasi D, Sauer M. Spotlight on biodiversity of microbial cell factories for glycerol conversion. Biotechnol Adv. 2019;37: 107395.
18. Dobson R, Gray V, Rumbold K. Microbial utilization of crude glycerol for the production of value-added products. J Ind Microbiol Biotechnol. 2012;39:217–26.
19. Li C, Lesnik KL, Liu H. Microbial conversion of waste glycerol from biodiesel production into value-added products. Energies. 2013;6:4739–68.
20. Papanikolaou S, Fakas S, Fick M, Chevalot I, Galiotou-Panayotou M, Komaitis M, Marc I, Aggelis G. Biotechnological valorisation of raw glycerol discharged after bio-diesel (fatty acid methyl esters) manufacturing process: Production of 1,3-propanediol, citric acid and single cell oil. Biomass Bioenergy. 2008;32:60–71.
21. Ahn J, Sang B, Um Y. Butanol production from thin stillage using *Clostridium pasteurianum*. Bioresource Technol. 2011;102:4934–7.
22. Cho S, Kim T, Woo HM, Kim Y, Lee J, Um Y. High production of 2,3-butanediol from biodiesel-derived crude glycerol by metabolically engineered *Klebsiella oxytoca* M1. Biotechnol Biofuels. 2015;8:146.
23. Liang Y, Cui Y, Trushenski J, Blackburn JW. Converting crude glycerol derived from yellow grease to lipids through *yeast* fermentation. Bioresource Technol. 2010;101:7581–6.
24. Pyle DJ, Garcia RA, Wen Z. Producing docosahexaenoic acid (DHA)-rich algae from biodiesel-derived crude glycerol: effects of impurities on DHA production and algal biomass composition. J Agric Food Chem. 2008;56:3933–9.
25. Zhang A, Liu H, Huang S, Fu Y, Fang B. Metabolic profiles analysis of 1,3-propanediol production process by *Clostridium butyricum* through repeated batch fermentation coupled with activated carbon adsorption. Biotechnol Bioeng. 2018;115:684–93.
26. Athalye SK, Garcia RA, Wen Z. Use of biodiesel-derived crude glycerol for producing eicosapentaenoic acid (EPA) by the fungus *Pythium irregulare*. J Agric Food Chem. 2009;57:2739–44.
27. Liu H, Xu Y, Zheng Z, Liu D. 1,3-Propanediol and its copolymers: Research, development and industrialization. Biotechnol J. 2010;5:1137–48.
28. Zhang A, Huang S, Zhuang X, Wang K, Yao C, Fang B. A novel kinetic model to describe 1,3-propanediol production fermentation by *Clostridium butyricum*. Aiche J. 2019;65: e16587.
29. Wang X, Zhou J, Sun Y, Xiu Z. Bioconversion of raw glycerol from waste cooking-oil-based biodiesel production to 1,3-propanediol and lactate by a microbial consortium. Front Bioeng Biotechnol. 2019;7:14.
30. Lee JH, Jung M, Oh M. High-yield production of 1,3-propanediol from glycerol by metabolically engineered *Klebsiella pneumoniae*. Biotechnol Biofuels. 2018;11:104.
31. Ju J, Wang D, Heo S, Kim M, Seo J, Kim Y, Kim D, Kang S, Kim C, Oh B. Enhancement of 1,3-propanediol production from industrial by-product by *Lactobacillus reuteri* CH53. Microb Cell Fact. 2020;19:6.
32. Zhou J, Shen J, Wang X, Sun Y, Xiu Z. Stability and oscillatory behavior of microbial consortium in continuous conversion of crude glycerol to 1,3-propanediol. Appl Microbiol Biotechnol. 2018;102:8291–305.
33. Zhang A, Zhu K, Zhuang X, Liao L, Huang S, Yao C, Fang B. A robust soft sensor to monitor 1,3-propanediol fermentation process by *Clostridium butyricum* based on artificial neural network. Biotechnol Bioeng. 2020;117:3345–55.
34. Wang X, Zhou J, Shen J, Zheng Y, Sun Y, Xiu Z. Sequential fed-batch fermentation of 1,3-propanediol from glycerol by *Clostridium butyricum* DL07. Appl Microbiol Biotechnol. 2020;104:9179–91.
35. Chatzifragkou A, Papanikolaou S, Dietz D, Doulgeraki AI, Nychas GE, Zeng A. Production of 1,3-propanediol by *Clostridium butyricum* growing on biodiesel-derived crude glycerol through a non-sterilized fermentation process. Appl Microbiol Biotechnol. 2011;91:101–12.
36. Van Ginkel S, Logan BE. Inhibition of biohydrogen production by undissociated acetic and butyric acids. Environ Sci Technol. 2005;39:9351–6.
37. Tee ZK, Jahim JM, Tan JP, Kim BH. Preeminent productivity of 1,3-propanediol by *Clostridium butyricum* JKT37 and the role of using calcium carbonate as pH neutraliser in glycerol fermentation. Bioresource Technol. 2017;233:296–304.
38. Jun S, Moon C, Kang C, Kong SW, Sang B, Um Y. Microbial fed-batch production of 1,3-Propanediol using raw glycerol with suspended

and immobilized *Klebsiella pneumoniae*. Appl Microbiol Biotechnol. 2010;161:491–501.
39. Wilkens E, Ringel AK, Hortig D, Willke T, Vorlop K. High-level production of 1,3-propanediol from crude glycerol by *Clostridium butyricum* AKR102a. Appl Microbiol Biotechnol. 2012;93:1057–63.
40. Petrache HI, Tristram-Nagle S, Harries D, Kučerka N, Nagle JF, Parsegian VA. Swelling of phospholipids by monovalent salt. J Lipid Res. 2006;47:302–9.
41. Xin B, Wang Y, Tao F, Li L, Ma C, Xu P. Co-utilization of glycerol and lignocellulosic hydrolysates enhances anaerobic 1,3-propanediol production by *Clostridium diolis*. Sci Rep. 2016;6:1–10.
42. Wei W, Ma G, Hu G, Yu D, Mcleish T, Su Z, Shen Z. Preparation of hierarchical hollow $CaCO_3$ particles and the application as anticancer drug carrier. J Am Chem Soc. 2008;130:15808–10.
43. Wang J, Chen J, Zong J, Zhao D, Li F, Zhuo R, Cheng S. Calcium carbonate/carboxymethyl chitosan hybrid microspheres and nanospheres for drug delivery. J Phys Chem C. 2010;114:18940–5.
44. Boyjoo Y, Pareek VK, Liu J. Synthesis of micro and nano-sized calcium carbonate particles and their applications. J Mater Chem A. 2014;2:14270–88.
45. Yang T, Ao Y, Feng J, Wang C, Zhang J. Biomineralization inspired synthesis of $CaCO_3$-based DDS for pH-responsive release of anticancer drug. Mater Today Commun. 2021;27: 102256.
46. Enyedi NT, Makk J, Kótai L, Berényi B, Klébert S, Sebestyén Z, Molnár Z, Borsodi AK, Leél-Őssy S, Demény A, Németh P. Cave bacteria-induced amorphous calcium carbonate formation. Sci Rep. 2020;10:8696.
47. Akiva-Tal A, Kababya S, Balazs YS, Glazer L, Berman A, Sagi A, Schmidt A. In situ molecular NMR picture of bioavailable calcium stabilized as amorphous $CaCO_3$ biomineral in crayfish gastroliths. Proc Natl Acad Sci. 2011;108:14763.
48. Tobler DJ, Rodriguez-Blanco JD, Dideriksen K, Bovet N, Sand KK, Stipp SLS. Citrate effects on amorphous calcium carbonate (ACC) structure, stability, and crystallization. Adv Funct Mater. 2015;25:3081–90.
49. Chong M, Rahim RA, Shirai Y, Hassan MA. Biohydrogen production by *Clostridium butyricum* EB6 from palm oil mill effluent. Int J Hydrog Energy. 2009;34:764–71.
50. Zhou J, Shen J, Wang X, Sun Y, Xiu Z. Metabolism, morphology and transcriptome analysis of oscillatory behavior of *Clostridium butyricum* during long-term continuous fermentation for 1,3-propanediol production. Biotechnol Biofuels. 2020;13:191.
51. Hirschmann S, Baganz K, Koschik I, Vorlop KD. Development of an integrated bioconversion process for the production of 1,3-propanediol from raw glycerol waters. Landbauforschung Völkenrode. 2005;55:261–7.
52. Rodriguez A, Wojtusik M, Ripoll V, Santos VE, Garcia-Ochoa F. 1,3-Propanediol production from glycerol with a novel biocatalyst *Shimwellia blattae* ATCC 33430: Operational conditions and kinetics in batch cultivations. Bioresour Technol. 2016;200:830–7.
53. Reimann A, Abbad-Andaloussi S, Biebl H, Petitdemange H. 1,3-Propanediol formation with product-tolerant mutants of *Clostridium butyricum* DSM 5431 in continuous culture: productivity, carbon and electron flow. J Appl Microbiol. 1998;84:1125–30.
54. Lan Y, Feng J, Guo X, Fu H, Wang J. Isolation and characterization of a newly identified *Clostridium butyricum* strain SCUT343-4 for 1,3-propanediol production. Bioproc Biosyst Eng. 2021;44:2375–85.
55. Thorwall S, Schwartz C, Chartron JW, Wheeldon I. Stress-tolerant non-conventional microbes enable next-generation chemical biosynthesis. Nat Chem Biol. 2020;16:113–21.
56. Pejin J, Radosavljević M, Mojović L, Kocić-Tanackov S, Djukić-Vuković A. The influence of calcium-carbonate and yeast extract addition on lactic acid fermentation of brewer's spent grain hydrolysate. Food Rev Int. 2015;73:31–7.
57. Yang P, Tian Y, Wang Q, Cong W. Effect of different types of calcium carbonate on the lactic acid fermentation performance of *Lactobacillus lactis*. Biochem Eng J. 2015;98:38–46.
58. Xue X, Li W, Li Z, Xia Y, Ye Q. Enhanced 1,3-propanediol production by supply of organic acids and repeated fed-batch culture. J Ind Microbiol Biotechnol. 2010;37:681–7.
59. Yin F, Zhang Y, Jiang J, Guo D, Gao S, Gao Z. Efficient docosahexaenoic acid production by *Schizochytrium* sp. via a two-phase pH control strategy using ammonia and citric acid as pH regulators. Process Biochem. 2019;77:1–7.
60. Zeng A. Pathway and kinetic analysis of 1,3-propanediol production from glycerol fermentation by *Clostridium butyricum*. Bioprocess Eng. 1996;14(4):169–75.
61. Zhou S, Li L, Perseke M, Huang Y, Wei J, Qin Q. Isolation and characterization of a *Klebsiella pneumoniae* strain from mangrove sediment for efficient biosynthesis of 1,3-propanediol. Sci Bull. 2015;60(5):511–21.
62. Ma B, Xu X, Zhang G, Wang L, Wu M, Li C. Microbial production of 1,3-propanediol by *Klebsiella pneumoniae* XJPD-Li under different aeration strategies. Appl Biochem Biotech. 2009;152(1):127–34.
63. Zhang A, Huang S, Zhuang X, Wang K, Yao C, Fang B. A novel kinetic model to describe 1,3-propanediol production fermentation by *Clostridium butyricum*. AIChE J. 2019;65(6): e16587.
64. Zhang C, Sharma S, Ma C, Zeng A. Strain evolution and novel downstream processing with integrated catalysis enable highly efficient coproduction of 1,3-propanediol and organic acid esters from crude glycerol. Biotechnol Bioeng. 2022;119(6):1450–2146.
65. Metsoviti M, Zeng A, Koutinas A, Papanikolaou S. Enhanced 1,3-propanediol production by a newly isolated *Citrobacter freundii* strain cultivated on biodiesel-derived waste glycerol through sterile and non-sterile bioprocesses. J Biotechnol. 2013;163(4):408–18.
66. Maina S, Kachrimanidou V, Ladakis D, Papanikolaou S, Castro A, Koutinas A. evaluation of 1,3-propanediol production by two *Citrobacter freundii* strains using crude glycerol and soybean cake hydrolysate. Environ Sci and Pollut R. 2019;26(35):35523–32.
67. Singh K, Ainala S, Park S. Metabolic engineering of *Lactobacillus reuteri* DSM 20,016 for improved 1,3-propanediol production from glycerol. Bioresource Technol. 2021;338: 125590.
68. Dietz D, Zeng A. Efficient production of 1,3-propanediol from fermentation of crude glycerol with mixed cultures in a simple medium. Bioproc Biosyst Eng. 2014;37(2):225–33.
69. Zhou J, Shen J, Jiang L, Sun Y, Mu Y, Xiu Z. Selection and characterization of an anaerobic microbial consortium with high adaptation to crude glycerol for 1,3-propanediol production. Appl Microbiol Biotechnol. 2017;101:5985–96.
70. Jiang L, Liu F, Yang W, Li C, Zhu B, Zhu X. Production of 1,3-propanediol and lactic acid from crude glycerol by a microbial consortium from intertidal sludge. Biotechnol Lett. 2021;43(3):711–7.
71. Benzerara K, Bolzoni R, Monteil C, Beyssac O, Forni O, Alonso B, Asta MP, Lefevre C. The gammaproteobacterium *Achromatium* forms intracellular amorphous calcium carbonate and not (crystalline) calcite. Geobiology. 2021;19:199–213.
72. Qian C, Ren X, Rui Y, Wang K. Characteristics of bio-$CaCO_3$ from microbial bio-mineralization with different bacteria species. Biochem Eng J. 2021;176: 108180.
73. Yan F, Zhang S, Guo C, Zhang X, Chen G, Yan F, Yuan G. Influence of stirring speed on the crystallization of calcium carbonate. Cryst Res Technol. 2009;44:725–8.
74. Ševčík R, Pérez-Estébanez M, Viani A, Šašek P, Mácová P. Characterization of vaterite synthesized at various temperatures and stirring velocities without use of additives. Powder Technol. 2015;284:265–71.
75. Sarkar O, Katakojwala R, Venkata MS. Low carbon hydrogen production from a waste-based biorefinery system and environmental sustainability assessment. Green Chem. 2021;23:561–74.
76. Petrognani C, Boon N, Ganigué R. Production of isobutyric acid from methanol by *Clostridium luticellarii*. Green Chem. 2020;22:8389–402.
77. Sivaramakrishnan R, Shanmugam S, Sekar M, Mathimani T, Incharoensakdi A, Kim S, Parthiban A, EdwinGeo V, Brindhadevi K, Pugazhendhi A. Insights on biological hydrogen production routes and potential microorganisms for high hydrogen yield. Fuel. 2021;291:120136.
78. Pachapur VL, Sarma SJ, Brar SK, Le Bihan Y, Buelna G, Verma M. Surfactant mediated enhanced glycerol uptake and hydrogen production from biodiesel waste using co-culture of *Enterobacter aerogenes* and *Clostridium butyricum*. Renew Energ. 2016;95:542–51.
79. RamKumar N, Anupama PD, Nayak T, Subudhi S. Scale up of biohydrogen production by a pure strain; *Clostridium butyricum* TM-9A at regulated pH under decreased partial pressure. Renew Energ. 2021;170:1178–85.
80. Park J, Kim D, Kim H, Wells GF, Park H. Granular activated carbon supplementation alters the metabolic flux of *Clostridium butyricum* for enhanced biohydrogen production. Bioresour Technol. 2019;281:318–25.

81. Wang Y, He L, Zhang Z, Zhao X, Qi N, Han T. Efficiency enhancement of H_2 production by a newly isolated maltose-preferring fermentative bio-hydrogen producer of *Clostridium butyricum* NH-02. J Energy Storage. 2020;30: 101426.
82. Liu N, Wang Q, Jiang J, Zhang H. Effects of salt and oil concentrations on volatile fatty acid generation in food waste fermentation. Renew Energ. 2017;113:1523–8.
83. Li Z, Yan L, Zhou J, Wang X, Sun Y, Xiu Z. Two-step salting-out extraction of 1,3-propanediol, butyric acid and acetic acid from fermentation broths. Sep Purif Technol. 2019;209:246–53.
84. Wood JM. Bacterial responses to osmotic challenges. J Gen Physiol. 2015;145:381–8.
85. Hosotani Y, Noviyanti F, Koseki S, Inatsu Y, Kawasaki S. Growth delay analysis of high-salt injured *Escherichia coli* O157:H7 in fermented soybean paste by real-time PCR and comparison of this method with other estimation methods. LWT. 2018;96:426–31.

Publisher's Note